

Electronic Supplementary Material (ESI) for Soft Matter.
This journal is © The Royal Society of Chemistry 2018

Supporting Information

Rapidly Tunable and Highly Reversible Bio-Inspired Dry Adhesion for Transfer Printing in Air and Vacuum

Changhong Linghu,^a Chengjun Wang,^a Nuo Cen,^b Jiaming Wu,^c Zhengfeng Lai^d and Jizhou Song^{*a}

^a Department of Engineering Mechanics, Soft Matter Research Center, and Key Laboratory of Soft Machines and Smart Devices of Zhejiang Province, Zhejiang University, Hangzhou 310027, China. E-mail: jzsong@zju.edu.cn

^b Faculty of Engineering, Zhejiang University, Hangzhou 310027, China.

^c Department of Mechatronic Engineering, Zhejiang University, Hangzhou 310027, China.

^d Department of Information Science and Electronic Engineering, Zhejiang University, Hangzhou 310027, China.

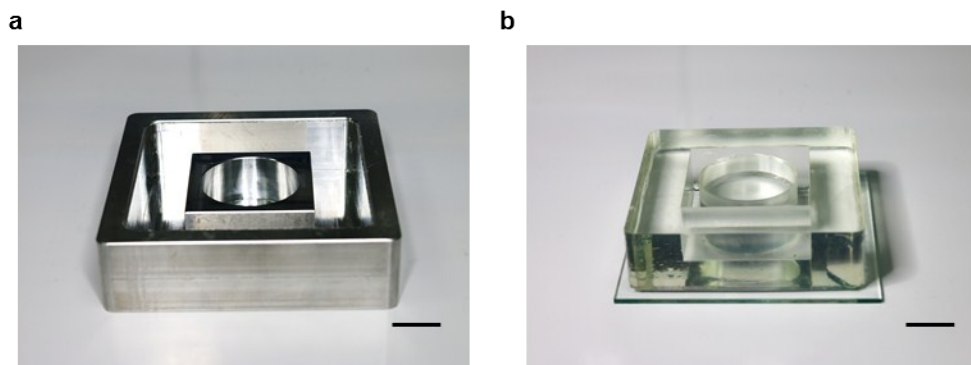


Fig. S1 Photograph of (a) the aluminum mold and (b) the PDMS positive mold. The scale bar corresponds to 20 mm.



Fig. S2 Photography of the pull test equipment. The home-made pull test equipment consists of a Materials Testing System (Model 5944, INSTRON), a two-axis manual tip/tilt platform and a permanent magnet. The bio-inspired stamp is lowered and raised by the linear stage of the tester in displacement control, and the in-line load cell measures the force on the glass substrate. The two-axis manual tip/tilt platform facilitates alignment between the stamp and the glass substrate. The gradient magnetic field is provided by a permanent NdFeB magnet and the magnitude of the magnetic pressure is controlled by changing the distance between the magnet and the glass substrate.

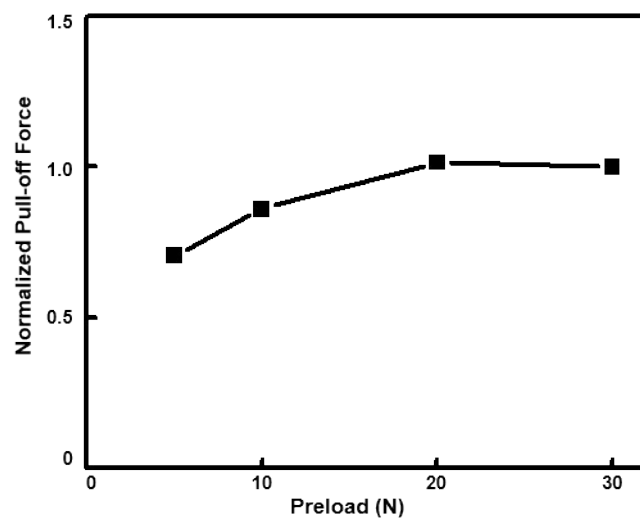


Fig. S3 Dependence of pull-off force on the applied preload ($V_r = 1000 \text{ um/s}$ and $p_m = 0$). The pull-off force is normalized by its maximum value (corresponds to the 30 N preload). The pull-off force increases with the preload until a plateau is reached at an applied preload of 30 N, which is used in the pull tests later.

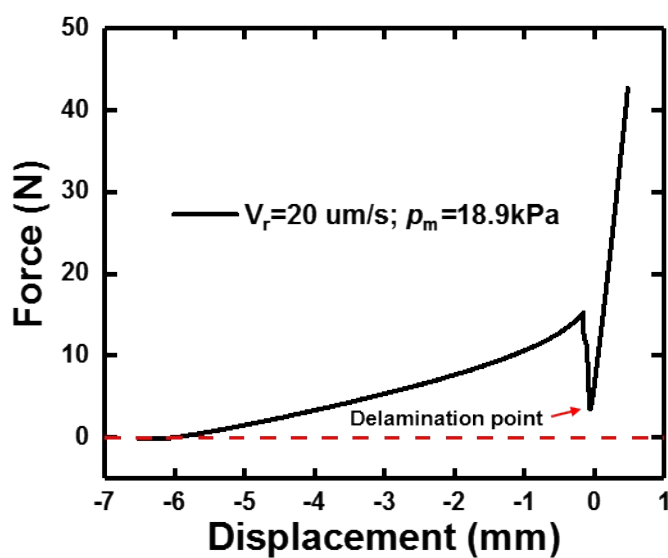


Fig. S4 Force-displacement curve with the elevated magnetic pressure and the low retraction speed. $V_r=20$ $\mu\text{m/s}$ and $p_m = 18.9$ kPa. The pull force remains positive, which means that the net force the stamp applied on the ink is a pressure (instead of an adhesion).

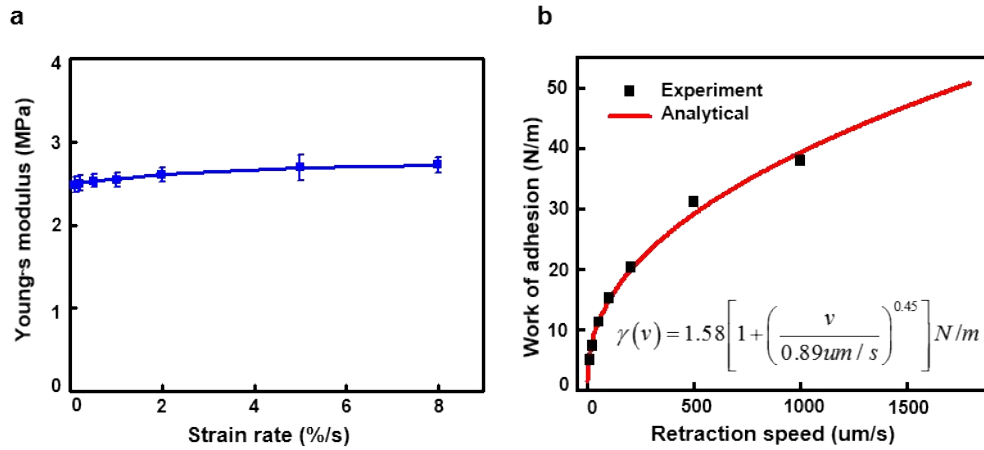


Fig. S5 Young's modulus of the stamp and work of adhesion of the stamp/glass interface.

PDMS is viscoelastic such that its Young's modulus and work of adhesion are rate dependent.

(a) The Young's modulus of PDMS at different strain rates. The stamp reservoir and the stamp membrane are made of PDMS of the same crosslinking ratio (10:1) and baked under the same temperature for the same time (75°C, 4h). Thus, the Young's moduli of the stamp reservoir and the stamp membrane are the same ($E_R = E_M$). The measured Young's modulus of PDMS changes from 2.48 MPa to 2.69 MPa for the strain rate from 0.05%/s-5%/s, corresponding the retraction speed from 10 μ m/s to 1000 μ m/s. **(b)** The work of adhesion between the stamp membrane and the glass substrate versus the retraction speed. The work of adhesion between the stamp membrane and the glass substrate is obtained from pull tests for different retraction speeds, and is fitted into the typical power law of the work of adhesion of a viscoelastic material.

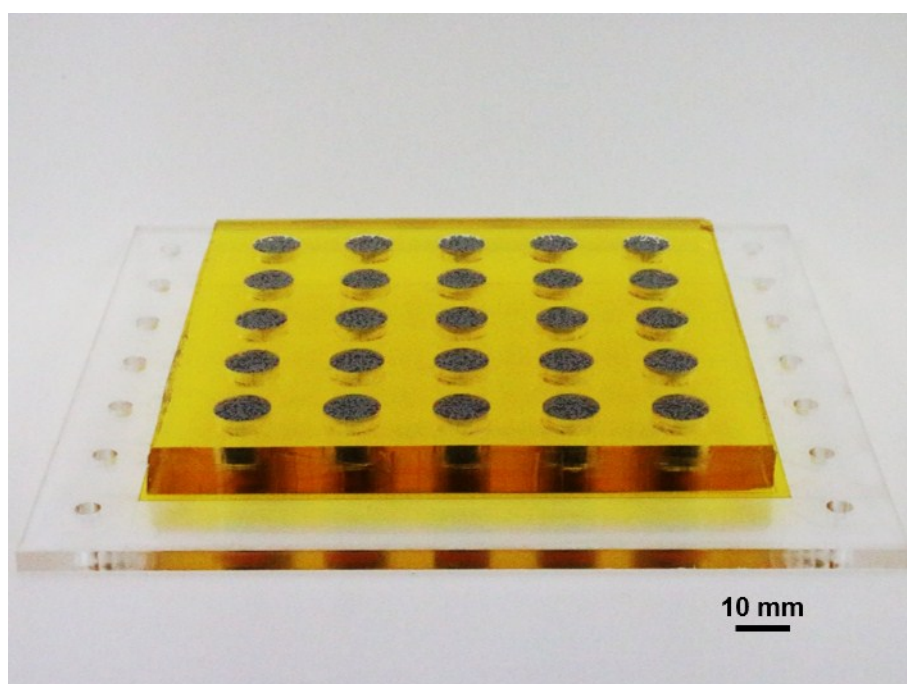


Fig. S6 Photography of the magnet-controlled stamp with 5×5 reservoir arrays for selective printing. Reservoir height: 8 mm, reservoir diameter: 10 mm, center to center distance of the reservoirs: 20 mm. Scale bar: 10 mm

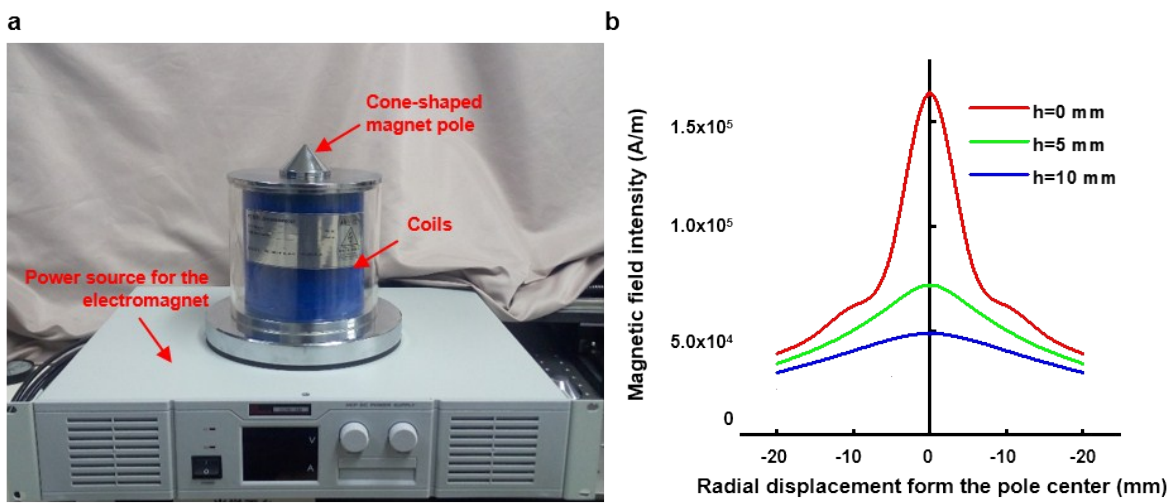


Fig. S7 The electromagnet with a cone-shaped pole for selective printing. (a) Photography of the electromagnet and (b) the magnetic field around the magnetic pole, the magnetic field is focused around the cone-shaped magnet pole. ‘ h ’ is the vertical distance from the magnetic pole tip.

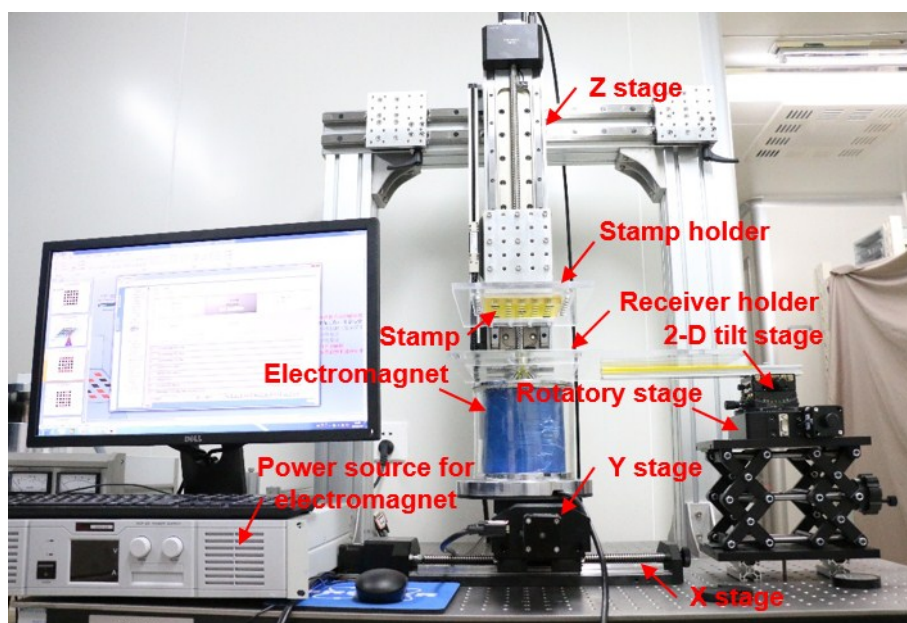


Fig. S8 Photography of the automated transfer printing platform. The platform consists of a stamp holder, receiver holder, a Z stage to move the stamp up and down, a X and Y stage for electromagnet movement, a 2-D tip/tilt stage and a rotatory stage for alignment between the stamp and the receiver.

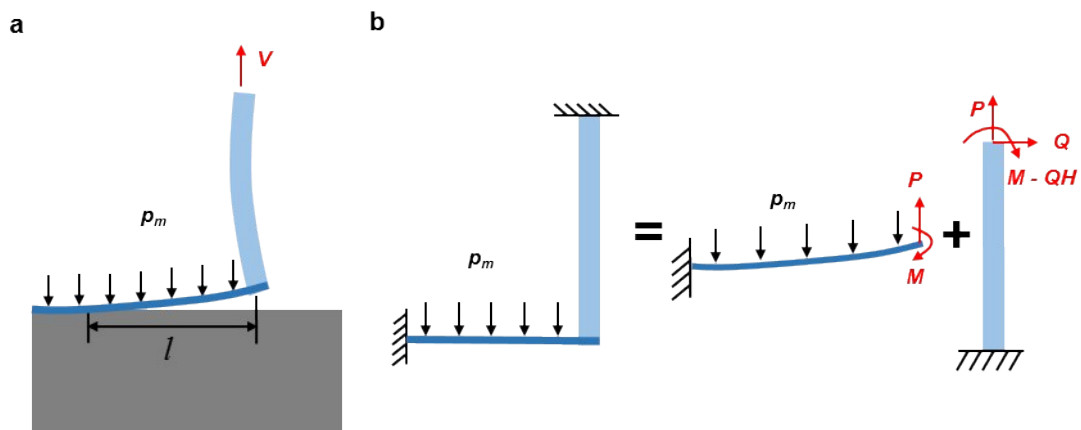


Fig. S9 Mechanics model for the partial delamination configuration. (a) Illustration of the partial delamination configuration of the magnetically actuated aphid-inspired stamp. (b) A double clamped L beam subjected to the magnetic pressure p_m on the bottom beam and the applied displacement V on the top of the vertical beam is used to model the system during the partial delamination stage. This is a statically indetermined system and can be solved by the superposition of the solutions for the following two problems: (1) a horizontal cantilever beam subjected to a uniform pressure p_m on the bottom, a concentrated force P and a moment M at the right end; (2) a vertical cantilever beam clamped at one end and subjected to a lateral load Q , a concentrated force P and a moment at the other end.

Note S1. Mechanics model

The potential energy of the partial delaminated system is given by $\Pi_2 = U - W + \Gamma$, in which U is the strain energy, $W = -\int_0^l p_m w dx$ is the external work done by p_m and $\Gamma = \gamma l$ is the adhesive energy of the interface. The reaction forces P and M in Eq. (2), which are functions of the applied displacement V and the delamination length l , can be obtained from the equilibrium of the double clamped L-shape beam subjected to the magnetic pressure p_m and the applied displacement V (shown in Fig. S9a) as¹

$$\left\{ \begin{array}{l} P(l, p_m, V) = (E_R A_R) \left[\frac{\frac{V}{H} \frac{E_M I_M}{E_R I_R} \frac{E_R I_R}{E_R A_R H^2} \left(\frac{l}{H} + \frac{1}{4} \frac{E_M I_M}{E_R I_R} \right) + \frac{1}{24} \frac{p_m H}{E_R A_R} \frac{l^4}{H^4} \left(\frac{l}{H} + \frac{3}{4} \frac{E_M I_M}{E_R I_R} \right)}{\frac{E_M I_M}{E_R I_R} \frac{E_R I_R}{E_R A_R H^2} \left(\frac{l}{H} + \frac{1}{4} \frac{E_M I_M}{E_R I_R} \right) + \frac{1}{12} \frac{l^3}{H^3} \left(\frac{l}{H} + \frac{E_M I_M}{E_R I_R} \right)} \right] \\ M(l, p_m, V) = (E_R A_R H) \left(\frac{\frac{1}{2} \frac{P}{E_R A_R} \frac{l^2}{H^2} - \frac{1}{6} \frac{p_m H}{E_R A_R} \frac{l^3}{H^3}}{\frac{l}{H} + \frac{1}{4} \frac{E_M I_M}{E_R I_R}} \right) \end{array} \right. \quad (S1)$$

The equilibrium of the stamp gives the pull force as¹

$$P_{pull} = 4E_R \frac{V}{H} A_R (L + A_R) - p_m \pi L^2. \quad (S2)$$

The pull force reaches its maximum value (i.e., the pull-off force) when the applied displacement reaches the critical displacement V_{crit} , which can be obtained from $\Pi_1 = \Pi_2$, such that

$$F_{pull-off} = 4E_R \frac{V_{crit}}{H} A_R (L + A_R) - p_m \pi L^2. \quad (S3)$$

Distributing the pull-off force on the adhesion area gives the adhesion strength of the interface as

$$p_a = \frac{V_{crit}}{H} \frac{E_R A_R}{(L + A_R)} - \frac{\pi p_m L^2}{4(L + A_R)^2} = E_R \frac{V_d}{H} \frac{A_R}{(L + A_R)}, \quad (S4)$$

where $V_d = V_{crit} - p_m \pi L^2 H / [4E_R A_R (L + A_R)]$ is the delamination displacement representing the relative displacement between that corresponding to zero-load and the critical displacement V_{crit} .

Legends for movies S1 to S5

Movie S1: Comparison of the Transfer Printing Process with/without Magnetic Field. This movie recorded and compared the transfer printing process of a silicon wafer (4 inches in diameter and 1 mm in thickness) onto a ceramic substrate in air with magnetically actuated aphid-inspired adhesive under three transfer printing modes: contact mode without (Segment 1) and with (Segment 2) magnetic field and non-contact mode with magnetic field (Segment 3). Speed control alone failed to release the silicon wafer even under a slow retraction speed (100 $\mu\text{m/s}$), and the active control of the adhesion via **the** magnetic field enabled successful transfer printing both in contact and non-contact modes in a quick and reliable manner. It demonstrates the reliability and quickly responsive characteristics of this transfer printing method.

Movie S2: Transfer Printing of a Stack of Silicon Wafers in the Air. This movie recorded the transfer printing process of a stack of silicon wafers in the air. It demonstrates the high manipulation efficiency and alignment accuracy of this transfer printing method.

Movie S3: Transfer Printing of a Stack of Silicon Wafers in Vacuum. This movie recorded the transfer printing process of a stack of silicon wafers in vacuum. It further demonstrates the capability in **the vacuum** of this transfer printing method.

Movie S4: Sequentially selective printing of five silicon platelets. This movie recorded the printing process of five selected silicon platelets from the all inked 5×5 array. It demonstrates the unique selective printing capabilities enable by a localized magnetic field.

Movie S5: Pattern printing by the scanning of a localized magnetic field. This movie recorded the patterned printing of the 'Z', 'J' and 'U' letters onto three PDMS substrates enabled by the scanning of the localized magnetic field. It further demonstrates that the printed pattern can be programmed as wish and deployed rapidly.

References

1. A. Carlson, S. Wang, P. Elvikis, P. Ferreira, Y. Huang and J. A. Rogers, *Active, Programmable Elastomeric Surfaces with Tunable Adhesion for Deterministic Assembly by Transfer Printing*, 2012.